Proc. Natl. Acad. Sci. USA
Vol. 88, pp. 9603–9607, November 1991
Biochemistry

Membrane topology analysis of *Escherichia coli* mannitol permease by using a nested-deletion method to create *mtlA–phoA* fusions

(bacterial phosphotransferase system/*phoA* fusions/membrane protein topology)

JANICE E. SUGIYAMA, SHEBA MAHMOODIAN, AND GARY R. JACOBSON*

Department of Biology, Boston University, 5 Cummington Street, Boston, MA 02215

Communicated by Hans Kornberg, August 2, 1991 (received for review July 4, 1991)

ABSTRACT **The *Escherichia coli* mannitol permease catalyzes the concomitant transport and phosphorylation of D-mannitol. This 68-kDa protein consists of a membrane-bound, N-terminal domain involved in mannitol binding and translocation and a C-terminal, cytoplasmic domain responsible for mannitol phosphorylation. Secondary-structure prediction methods suggest that the N-terminal half of the permease spans the membrane approximately seven times in α-helical segments, but these data cannot conclusively predict the structure. We have used gene fusions between *mtlA* (encoding the permease) and *'phoA* (encoding alkaline phosphatase lacking its signal sequence) to further investigate the topology of the mannitol permease. Initially, fusions were constructed by using a λTn*phoA* vector and *in vitro* cloning of *'phoA* into naturally occurring restriction sites in *mtlA*. However, the former method gave severe problems with insertion "hot-spots" in our vector systems, and the latter method was limited by the number of useful restriction sites. Therefore, we developed a nested-deletion method for creating *mtlA–phoA* fusions. *'phoA* was first cloned downstream from the part of *mtlA* encoding the membrane-bound half of the permease. This construct was then treated with the appropriate restriction enzymes and with exonuclease III to create random fusions. An analysis of >40 different fusion clones constructed by these methods provides strong evidence for six membrane-spanning regions in the mannitol permease with three relatively short periplasmic loops and two large cytoplasmic loops in the membrane-bound half of the protein.**

The *Escherichia coli* mannitol permease is a carbohydrate-specific enzyme II of the phospho*enol*pyruvate-dependent phosphotransferase system, a common mechanism for the concomitant transport and phosphorylation of carbohydrates in anaerobic and facultatively anaerobic bacteria (for review, see ref. 1). This protein also acts as a primary chemotactic receptor for mannitol. The mannitol permease is a 68-kDa protein comprised of an N-terminal, membrane-bound domain consisting of ≈334 aminoacyl residues and a C-terminal cytoplasmic domain (residues 335–637) responsible for its phosphorylation functions. Because the membrane-bound domain is sufficient to bind mannitol, that domain is likely to contain the substrate-recognition site and also the channel that traverses the membrane. Structural prediction methods suggested that the N-terminal half of the mannitol permease may consist of seven transmembrane α-helical regions (2). However, these methods are ambiguous, and derived models must be tested experimentally (3).

The membrane-bound domain of the mannitol permease is refractory to proteolytic digestion (4); therefore, we used the *phoA* fusion technique of Manoil and Beckwith (5) to investigate the topology. This method involves fusing the gene *'phoA*, encoding alkaline phosphatase (AP) but lacking its signal sequence, to various parts of a gene encoding a bacterial-membrane protein (in this case, *mtlA*). AP activities in cells expressing hybrid proteins can then be used to map the membrane topology of the target protein. Because we encountered difficulties with insertion "hot-spots" using λTn*phoA*, we developed an *in vitro*, nested-deletion method to create *mtlA–phoA* fusions. This method yielded many different, in-frame fusions that were easy to identify and randomly spaced within the 5′ half of the gene. Activities of these fusion proteins strongly support a model for the mannitol permease consisting of six transmembrane regions in the N-terminal half of the protein. Furthermore, this method is generally applicable and avoids limitations inherent in some other methods.

MATERIALS AND METHODS

Chemicals and Enzymes. [γ-^{32}P]dATP (800 Ci/mmol; 1 Ci = 37 GBq) was from DuPont/NEN. T4 polynucleotide kinase and exonuclease III (exo III) were from New England Biolabs; DNA polymerase I Klenow fragment, calf intestinal alkaline phosphatase, and S1 nuclease were from United States Biochemical; restriction enzymes were from New England Biolabs, United States Biochemical, or American Allied Biochemical (Aurora, CO). Chemicals were from Sigma. Oligonucleotides were synthesized on a MilliGen (Bedford, MA) model 6500 instrument by D. Tolan (Boston University, Boston).

Bacteria, Plasmids, and Phage. *E. coli* strains used were CC118 [*araD139* Δ(*ara, leu*)*7697* Δ*lacX74 phoA*Δ*20 galE galK thi rpsE rpoB argE*$_{am}$ *recA1*], provided by C. Manoil (University of Washington, Seattle); LJ921 (CC118; *mtlA70*), provided by M. Saier (University of California, San Diego, La Jolla); and GM1684 [F′-*lacI*^{q} *M15 pro*$^+$/*dam-4* Δ(*lac-pro*)*XIII thi-1 glnV44* (*relA1*)], provided by M. Marinus (University of Massachusetts Medical School, Worcester). Plasmids used were pUC19 and pBR322 (6, 7), pGJ9 [pACYC184 derivative containing *mtlA* (8)], and plasmids pCH39 and pCH40 [pBR322 derivatives provided by A. Wright (Tufts University Medical School, Boston)], containing *bla–phoA* fusions with a *Pst* I site at the fusion junction (9). λTn*phoA* was as described (10) and provided by C. Manoil.

Assay. Mid-exponential phase cultures of CC118 or LJ921 cells containing fusion plasmids were grown in Luria broth and assayed for their ability to hydrolyze *p*-nitrophenyl phosphate (11).

Construction of pStel. The *mtlA* gene from pGJ9 was cloned into the *tet* gene of pBR322 by using *Hin*dIII and *Bam*HI sites. The resulting vector, pStel (Fig. 1), was used as the parent vector for constructing most *mtlA–phoA* fusions.

The publication costs of this article were defrayed in part by page charge payment. This article must therefore be hereby marked "*advertisement*" in accordance with 18 U.S.C. §1734 solely to indicate this fact.

Abbreviations: XP, 5-bromo-4-chloro-3-indolyl phosphate; AP, alkaline phosphatase; exo III, *Escherichia coli* exonuclease III.

*To whom reprint requests should be addressed.

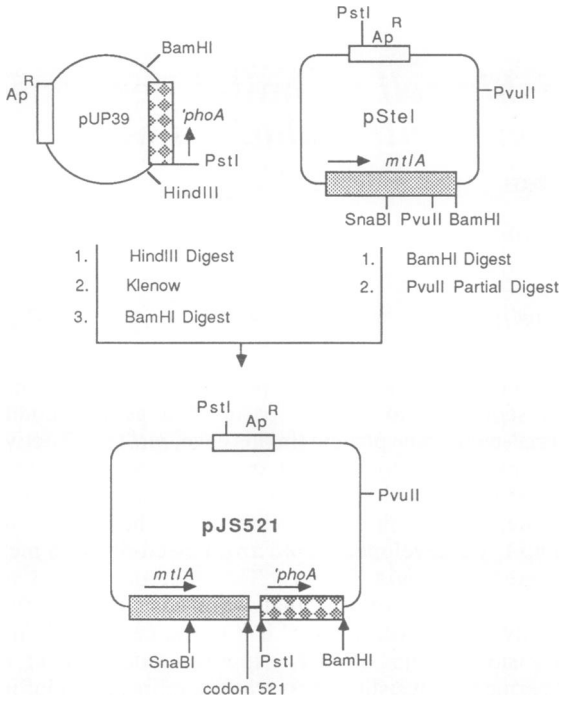

FIG. 1. Construction of pJS521. This construct has *'phoA* (bar of hatched squares) fused downstream of *mtlA* region encoding membrane-associated domain (stippled bar). *mtlA* codons 521–637 were removed by digesting pStel (see text) with *Bam*HI, followed by partial *Pvu* II digestion. pUP39 was first digested with *Hin*dIII and treated with Klenow fragment to create blunt ends. *'phoA* was then removed by *Bam*HI digestion and ligated to the appropriate pStel fragment.

Isolation of *in Vivo mtlA–phoA* Fusions. Fusions were constructed by infecting LJ921 cells, containing either pGJ9 or pStel, with λTn*phoA* and screening them on selective agar plates containing 5-bromo-4-chloro-3-indolyl phosphate (XP), as described by Manoil and Beckwith (10). Blue colonies were isolated and streaked onto MacConkey agar plates containing 0.25% mannitol, kanamycin at 40 μg/ml, and chloramphenicol at 30 μg/ml (pGJ9) or ampicillin at 40 μg/ml (pStel) to identify fusions into *mtlA*. Plasmid DNA was prepared from white colonies and analyzed by restriction mapping and sequencing.

***In Vitro* Construction of *mtlA–phoA* Fusions.** The *'phoA* gene from plasmids pCH39 and pCH40 was subcloned into pUC19. *Pst* I–*Xho* I fragments containing *'phoA* were removed from the pCH vectors and inserted into pUC19 at the *Pst* I and *Sal* I sites, creating vectors pUP39 and pUP40. *'phoA* was removed from pUP vectors with *Hin*dIII and *Bam*HI digestions to construct the following five *in vitro mtlA–phoA* fusions. (*i*) pJS12 was created by digesting pStel completely with *Bam*HI and partially with *Hin*dIII (one site lies within codon 12 of *mtlA*) to remove *mtlA* codons 12–637. This region was replaced by *'phoA* from pUP39. (*ii*) pJS69 was constructed by replacing codons 69–637 of the *mtlA* gene with *'phoA*. Two complementary 41-mer oligonucleotides were used that encoded residues 56–68 of the mannitol permease and produced *Bcl* I and *Hin*dIII sites at the ends. pStel was first passaged through GM1684 cells (*dam*$^-$) and digested with *Bcl* I, which cuts within codon 56. *Bcl* I-linearized pStel was hybridized and ligated with the oligonucleotides and then digested with *Bam*HI and ligated with the *'phoA* fragment from pUP40. (*iii*) pJS126 was made by replacing codons 126–637 with *'phoA*. There are three *Acc* I sites in pStel; one lies within codon 118. Codons 118–637 were removed by digesting pStel with *Bam*HI, followed by partial *Acc* I digestion. *'phoA* was removed from pUP40 with a *Hin*dIII and *Bam*HI digest and ligated to two complementary 23-mer and 25-mer oligonucleotides with *Acc* I and *Hin*dIII ends, which include codons 118–125. This modified *'phoA* fragment was inserted into the pStel vector containing *mtlA* codons 1–125. (*iv*) pJS233 was constructed by replacing codons 233–637 with *'phoA*. There are two *Afl* III sites in pStel; one lies within codon 233. pStel was first linearized with a *Bam*HI digest, then partially digested with *Afl* III, and ligated to *'phoA* (removed from pUP39). Only the *Bam*HI-digested ends were compatible, so the *Hin*dIII and *Afl* III 5′-overhanging ends were blunt-ended by filling in the 3′-recessed strands; these ends were subsequently ligated. (*v*) pJS521 was constructed by fusing *'phoA* to *mtlA* codons 1–520. There are two *Pvu* II sites within pStel; one lies within codon 521. *Bam*HI-linearized pStel was partially digested with *Pvu* II to remove codons 521–637. pUP39 was first treated with *Hin*dIII, the 3′-recessed ends were filled in, and the *'phoA* fragment was removed by digestion with *Bam*HI. This procedure was followed by ligation to the pStel fragment (Fig. 1).

***In Vitro* Construction of Gene Fusions by exo III-Nested Deletion.** pJS521 was used to construct a series of fusion plasmids by nested deletions in the *mtlA* gene. exo III digests linear DNA having 5′-overhanging ends or blunt ends, whereas 3′-overhanging ends are resistant to nuclease action (12). A *Sna*BI site lies within codon 377. This enzyme creates a blunt end, which can then be used as a substrate for exo III. *Pst* I, which creates a 3′ overhang, was used to protect bases from exo III digestion. Two *Pst* I sites occur in pJS521; one lies at the 5′ end of *'phoA*. For the nested-deletion experiments, pJS521 was linearized with *Sna*BI and then partially digested with *Pst* I.

The exo III digestion reaction proceeds at ≈400 bases per min at 35°C (12, 13). Restriction-digested DNA was resuspended in exo III buffer and kept at 35°C. exo III was added to pJS521, aliquots were removed at 20-s intervals, and added to tubes on ice containing S1 nuclease. When all time points had been taken, tubes were removed from ice and incubated at room temperature. exo III-digested DNA was filled-in with deoxynucleotides and Klenow fragment, the ends were ligated together, and recircularized DNA was transformed into CC118 cells. Transformants producing in-frame AP were selected on Luria broth plates containing ampicillin at 50 μg/ml and XP at 40 μg/ml. *mtlA–phoA* fusions were confirmed by DNA sequencing.

DNA Sequence Analysis of *phoA* Fusions. Double-stranded *mtlA–phoA* plasmid DNA was sequenced according to the Sequenase version 2.0 sequencing protocol (United States Biochemical). The sequencing primer for the *in vivo* fusions hybridized at the 5′ end of *'phoA*. A second primer for sequencing *in vitro* fusions hybridized at a site ≈65 bases downstream from the first primer.

RESULTS

***In Vivo phoA* Fusions.** *In vivo* fusions were made by infecting CC118 cells carrying pGJ9 with λTn*phoA*. Cells carrying in-frame fusion plasmids were selected on agar plates containing the appropriate antibiotics and XP. These cells produced two types of colonies: those containing high-activity fusion proteins were dark blue, and those containing low-activity proteins were lighter blue. Although in theory, AP on the cytoplasmic side of the membrane should be inactive, these fusion proteins had sufficient activities to produce light-blue colonies.

Approximately 700 fusion clones isolated by this method that produced AP were screened on MacConkey-mannitol plates and by restriction analysis to identify fusions into the *mtlA* gene. This analysis was followed by sequencing to

determine the fusion location. Five different *mtlA–phoA* fusions were identified in codons 152, 157, 169, 209, and 264. However, two hot-spots were found. At least 21 of 35 *mtlA–phoA* fusions were found within codon 157 of the *mtlA* gene, whereas codon 169 was the site of an additional four fusions. One fusion was isolated with the *phoA* gene inserted in the opposite orientation and was used as a negative control for the AP activity assay. Although transposition of Tn*phoA* was expected to occur randomly, intrinsic properties seemed to influence insertion of the *phoA* gene, possibly the result of pGJ9 sequences near the insertion hot-spots and/or secondary-structure effects.

To attempt to overcome these difficulties, a new vector, pStel, a pBR322 derivative containing the *mtlA* gene, was constructed and used in place of pGJ9. In-frame AP fusion clones (770) were purified and screened. The fusion junctions of 45 likely *mtlA–phoA* fusion plasmids were sequenced. Only two new fusions were identified within codons 56 and 223. An additional fusion was found at a site also isolated with pGJ9 (codon 209). No fusions were found in the pGJ9 hot-spot (codon 157). The remainder of *phoA* fusion plasmids expressing active AP were *phoA* insertions into the 3′ end of the *bla* gene (≈50% of all fusion clones) and at the 5′ end of the *tet* gene (≈30% of all fusion clones). Insertions into the 3′ end of the *bla* gene apparently retained the ability to produce and export β-lactamase because they still grew on ampicillin plates and produced dark-blue colonies on XP plates. Although use of pStel circumvented some of the problems seen with pGJ9, *phoA* fusions within *bla* and *tet* predominated, which could not be counterselected by simple procedures.

***In Vitro phoA* Fusions.** To obtain fusions in other regions of *mtlA*, the *'phoA* gene was cloned directly into restriction sites within the *mtlA* gene, resulting in insertion of *'phoA* into *mtlA* codons 12, 69, 126, 233, and 521 (see *Materials and Methods*). Constructs were sequenced to ensure that fusions were at the correct site and that *phoA* was in the correct reading frame.

***mtlA–phoA* Fusions Using exo III-Nested Deletions.** To further saturate the N-terminal half of the mannitol permease with AP fusions, a technique was developed that created nested deletions in the *mtlA* gene (see *Materials and Methods*). exo III was incubated with pJS521 that had been digested with *Sna*BI and *Pst* I. Fifteen aliquots were taken at 20-s intervals and analyzed on an agarose gel (Fig. 2). The digested DNA was ligated and transformed into CC118 cells. Plasmids were obtained from blue transformants, and 92 appropriately sized plasmids were sequenced. Thirty-four of these plasmids were in-frame *phoA* fusions into the *mtlA* gene, ranging from insertions into codons 325–33. One fusion had the same insertion site as pJS69, which was constructed by direct cloning (see *Materials and Methods*). The remaining plasmids were either wild type or identical to one of the other *phoA* fusions.

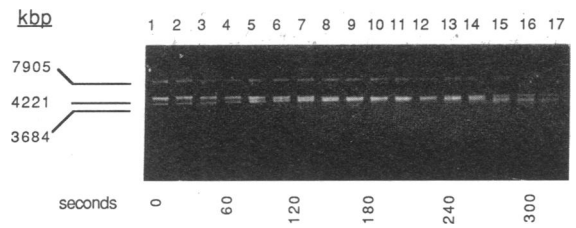

FIG. 2. exo III-nested deletion of pJS521. Complete *Sna*BI digestion followed by partial *Pst* I digestion produced four fragments of 7905, 4221, 3684, and 440 kilobase pairs (kbp) (lane 1). The 3684-kbp fragment has two *Pst* I ends and is resistant to exo III digestion. The 7905-kbp band (the desired fragment) results from *Pst* I cleavage of the *Sna*BI-linearized DNA only at the site immediately 5′ to *phoA*. *Sna*BI/*Pst* I-digested pJS521 was treated with exo III; aliquots were then removed at 20-s intervals and analyzed on the gel (lanes 2–17).

AP Activities of MtlA-PhoA Fusion Proteins. The fusions and their activities are listed in Table 1 and graphed relative to the amino acid sequence in Fig. 3. There are three regions within the first 325 amino acid residues with high activity (75–400 units per OD unit): residues 37–59, residues 144–174, and residues 286–311. These regions are bordered by areas of low AP activity (<20 units per OD unit). There is also a region (residues 91–93) that displays intermediate activity (>20 but <75 units per OD unit). When activities of these fusion proteins were superimposed on the seven-helix model of the

Table 1. MtlA–PhoA fusions obtained by three different methods

Fusion	Method of construction	Location*	AP activity,† units per OD unit
1 (pJS12)	*In vitro*	Phe-12	1
2	exo III	Ile-33	1
3	exo III	Phe-37	76
4	exo III	Gly-41	218
5	exo III	Leu-43	108
6	exo III	Lys-50	175
7	exo III	Pro-54	226
8	Tn*phoA*	Ile-56	169
9	exo III	Thr-57	160
10	exo III	Leu-59	146
11	exo III	Leu-63	1
12	exo III	Gly-68	4
13a (pJS69)	*In vitro*	Gly-69	<1
13b	exo III	Gly-69	6
14	exo III	Leu-71	4
15	exo III	Gly-74	2
16	exo III	Ala-82	3
17	exo III	Gly-91	20
18	exo III	Ala-92	45
19	exo III	Asp-93	50
20	exo III	Met-94	7
21	exo III	Ser-100	17
22	exo III	Trp-109	6
23 (pJS126)	*In vitro*	Phe-126	<1
24	exo III	Ile-144	90
25	exo III	Ala-146	119
26	exo III	Gly-151	90
27	Tn*phoA*	Pro-152‡	354
28	exo III	Ala-156	219
29	Tn*phoA*	Leu-157‡	320
30	exo III	Met-168	110
31	Tn*phoA*	Val-169‡	142
32	exo III	Leu-174	202
33a	Tn*phoA*	Leu-209‡	10
33b	Tn*phoA*	Leu-209	8
34	exo III	Asn-220	19
35	Tn*phoA*	Pro-223	<1
36	exo III	Met-225	7
37	exo III	Val-227	7
38 (pJS233)	*In vitro*	Phe-233	1
39	Tn*phoA*	Leu-264‡	5
40	exo III	Ile-286	239
41	exo III	Ile-300	225
42	exo III	Gly-310	227
43	exo III	Ala-311	248
44	exo III	Val-325	2
45 (pJS521)	*In vitro*	Leu-521	<1
46	Tn*phoA*	Inverted‡	<1

*Codon of *mtlA* into which *'phoA* is fused.
†AP activity is an average of two to seven values from independent determinations.
‡Fusion clones that used pGJ9 as parent plasmid; all other fusions were constructed in pStel.

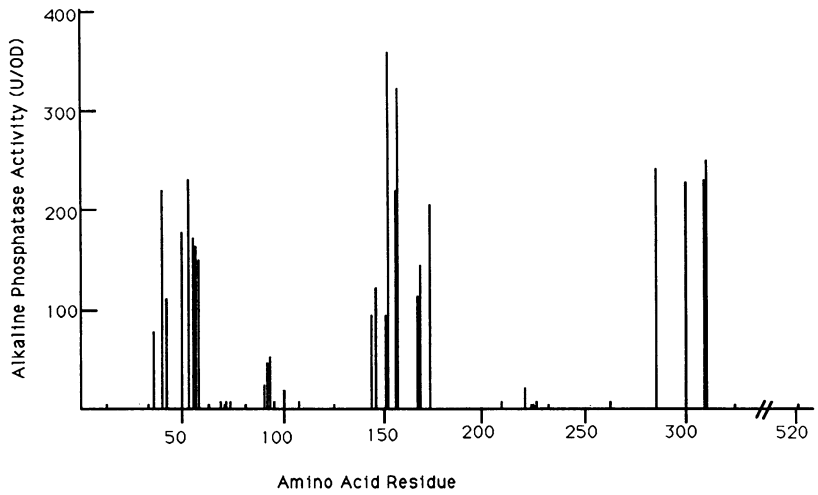

FIG. 3. AP activity plotted against residue location in the mannitol permease. U/OD, units per OD unit.

mannitol permease (2), results were compatible with the topology of residues ≈95–335 but not with residues 1–94 (Fig. 4*A*). A six-helix model (shown in Fig. 4*B*) is more strongly supported by the *phoA* fusion results.

DISCUSSION

In this report, we have applied the gene-fusion method of Manoil and Beckwith (5) to extensively investigate the membrane topology of the *E. coli* mannitol permease. Because we encountered fusion hot-spots in one *mtlA*-containing vector (pGJ9) using the *in vivo* λTn*phoA* technique, and many fusions generated with pStel were found in *tet* or *bla*, we developed a procedure that resulted in a high frequency of random fusions within the 5′ half of *mtlA*. Positions of the fusion junctions in plasmids isolated at various times of exo III digestion correlated well with the value of ≈400 bases digested per min (12, 13). Furthermore, most fusions constructed by this technique were different and could be identified easily by screening cells on XP-containing plates. Even cells carrying very low-activity fusions produced sufficient XP hydrolysis to distinguish them from the white colonies with no activity (e.g., out-of-frame fusions).

This method for producing *phoA* fusions has several advantages over the *in vivo* method with λTn*phoA*: rapidity, efficiency, and ease of screening fusions. This technique should be generally applicable if *'phoA* with a 5′ *Pst* I site (or other protecting site) can be cloned downstream from the gene of interest and an exo III-sensitive restriction site exists between the protecting site and the target gene.

The model for the mannitol permease based on the fusion results is shown in detail in Fig. 5 and differs from that previously proposed by us (2). Although all six transmembrane regions in Fig. 5 were predicted in the previous model, a seventh region (residues 79–97) is not predicted to traverse the membrane in the present model. Moreover, transmembrane regions 1 and 2 are proposed to have opposite orientations in the membrane compared with the earlier model (Fig. 4). Nevertheless, the present model is still consistent with the results from predictive and biochemical studies (2).

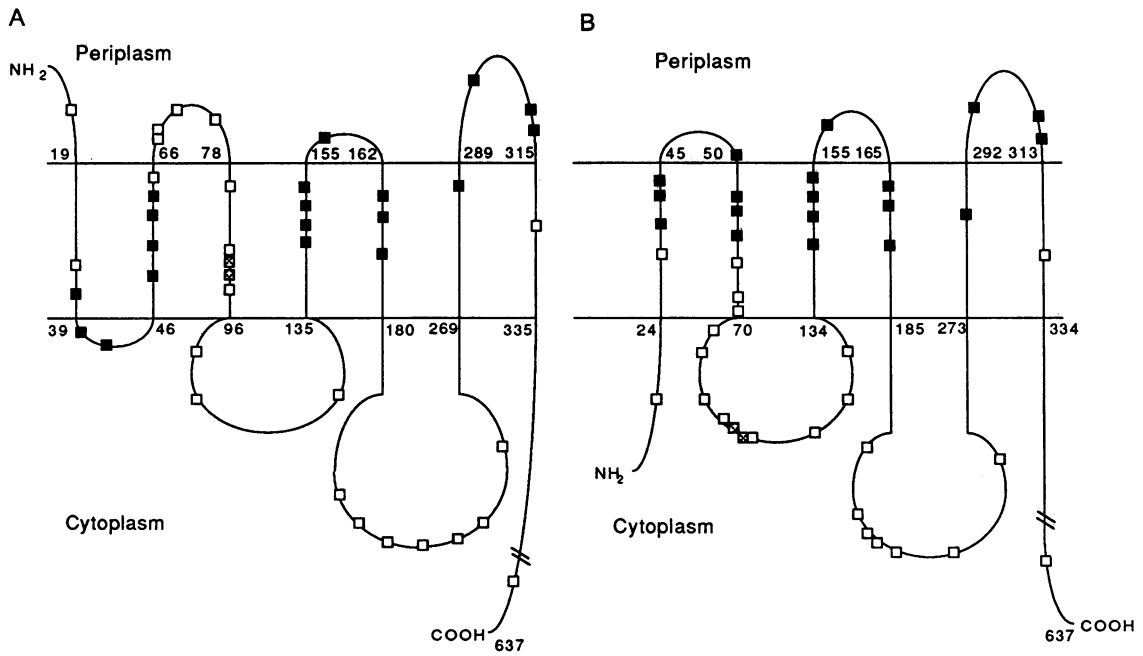

FIG. 4. Fusion activities superimposed on the previous (2) (*A*) and current (*B*) mannitol permease models. AP fusion locations are indicated with boxes. Fusions were grouped according to AP activity: □, low [<20 units per OD unit (U/OD)]; ⊠, intermediate (20–75 U/OD); and ■, high (>75 OD units). Residues at the membrane–aqueous interfaces are numbered.

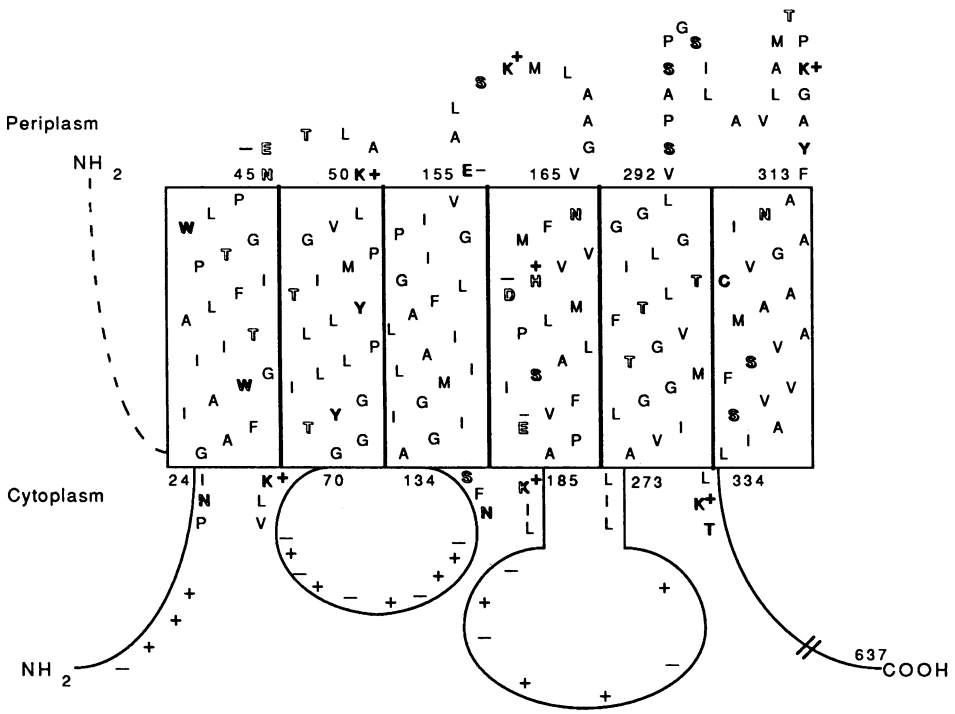

FIG. 5. Predicted model of the mannitol permease showing residue location. Residues are arranged in membrane-spanning regions in α-helical arrays. Polar and/or potential H-bonding residues are indicated by open symbols. Only charged residues and the first three residues at each cytoplasm and membrane interface are shown in the cytoplasmic region. Dashed line leading from N terminus to residue 24 indicates that the N-terminus location is unknown but is probably cytoplasmic (see text). Distribution of polar residues is quite uniform through the depth of the membrane, as expected for a hydrophilic channel-forming protein.

The midpoints of transmembrane regions in Fig. 5 were inferred from the activity results and from recent evidence that only ≈10 residues of an "outgoing" transmembrane region are sufficient to promote export when fused to AP, whereas 10 or 11 residues of an "incoming" transmembrane region are usually insufficient to anchor AP in the cytoplasm (14). The only potential anomaly in the activity profile of these fusions is a small region of low-to-intermediate activity within codons 91–93 (Fig. 3) now proposed to be cytoplasmic. However, the highest activity fusion within this region (fusion 20 within codon 93) had only 50 units of activity compared to at least 220 units for the highest activity fusions within proposed periplasmic loops. Also, fusion 21 within codon 94 (which introduces aspartate immediately N terminal to AP) had only seven units of activity. Because residues 79–92 comprise a relatively hydrophobic stretch previously proposed to be within the membrane (2), fusion of this region to AP apparently allows for some (inefficient) export. However, three facts make it likely that the region between residues 70 and 134 is either cytoplasmic or does not completely traverse the membrane: (*i*) fusion 21 has very low activity; (*ii*) the region between residues 98 and 134 is not predicted to be transmembrane by hydropathy analysis (2, 15); and (*iii*) the region around Cys-110 has been shown to be cytoplasmic (2).

The model of Fig. 5 has several notable features. (*i*) There are two large cytoplasmic loops in the N-terminal domain, whereas the three predicted periplasmic loops are all relatively short. (*ii*) The ratio of positively charged residues in cytoplasmic loops to those in periplasmic loops is 5:1, in accordance with the von Heijne "positive-inside" rule (16). This calculation assumes that the N-terminal 24 residues are cytoplasmic rather than transmembrane (a possibility shown by the dashed line in Fig. 5). At present, no convincing evidence exists to assign location of the N terminus. Although this region is not highly hydrophobic, it can form an amphipathic helix with a large hydrophobic moment (17) and could traverse the membrane as part of a bundle of amphipathic helices. (*iii*) A lysine residue is at or near the N-proximal end of all three cytoplasmic domains of the permease. Positively charged residues positioned in this manner have been hypothesized to aid in anchoring loops of transmembrane proteins in the cytoplasm (for review, see ref. 18).

Finally, only two of the predicted transmembrane regions (4 and 6) of the mannitol permease can form strongly amphipathic α-helices, and of the ≈120 residues predicted within the membrane, only 20 are polar and/or capable of forming hydrogen bonds with the polyol substrate (Fig. 5). Thus, this model limits the number of possible three-dimensional arrangements of transmembrane helices that could form a hydrophilic channel; it also limits the number of residues that could contribute to a channel/binding site. The model will, therefore, be useful in devising experiments to explore structure–function relationships in this part of the mannitol permease, which is undoubtedly involved in translocation of substrate.

We are grateful to Drs. D. Tolan, A. Wright, T. Gilmore, and C. Manoil, and to A. Capobianco for many helpful discussions. This research was supported by Public Health Service Grant GM28226 from the National Institute of General Medical Sciences.

1. Postma, P. W. & Lengeler, J. (1985) *Microbiol. Rev.* **49**, 232–269.
2. Jacobson, G. R. & Stephan, M. M. (1989) *FEMS Microbiol. Rev.* **63**, 25–34.
3. Lodish, H. F. (1988) *Trends Biochem. Sci.* **13**, 332–334.
4. Stephan, M. M. & Jacobson, G. R. (1986) *Biochemistry* **25**, 8230–8234.
5. Manoil, C. & Beckwith, J. (1986) *Science* **233**, 1403–1408.
6. Yanisch-Perron, C., Vieira, J. & Messing, J. (1985) *Gene* **33**, 103–119.
7. Sutcliffe, J. G. (1978) *Cold Spring Harbor Symp. Quant. Biol.* **43**, 77–90.
8. Grisafi, P., Scholle, A., Sugiyama, J., Briggs, C., Jacobson, G. R. & Lengeler, J. W. (1989) *J. Bacteriol.* **171**, 2719–2727.
9. Hoffman, C. S. & Wright, A. (1985) *Proc. Natl. Acad. Sci. USA* **82**, 5107–5111.
10. Manoil, C. & Beckwith, J. (1985) *Proc. Natl. Acad. Sci. USA* **82**, 8129–8133.
11. Brickman, E. & Beckwith, J. (1975) *J. Mol. Biol.* **96**, 307–316.
12. Henikoff, S. (1984) *Gene* **28**, 351–359.
13. Capobianco, A., Simmons, D. L. & Gilmore, T. (1990) *Oncogene* **5**, 257–266.
14. Calamia, J. & Manoil, C. (1990) *Proc. Natl. Acad. Sci. USA* **87**, 4937–4941.
15. Lee, C. A. & Saier, M. H., Jr. (1983) *J. Biol. Chem.* **258**, 10761–10767.
16. von Heijne, G. (1986) *EMBO J.* **5**, 3021–3027.
17. Saier, M. H., Jr., Werner, P. K. & Müller, M. (1989) *Microbiol. Rev.* **53**, 333–366.
18. Dalbey, R. E. (1990) *Trends Biochem. Sci.* **15**, 253–257.